A R C H I V E S O F M E T A L L U R G Y A N D M A T E R I A L S
Volume 58 2013 Issue 4
DOI: 10.2478/amm-2013-0141

G. SIWIEC*

THE KINETICS OF ALUMINIUM EVAPORATION FROM THE Ti-6Al-4V ALLOY

KINETYKA PAROWANIA ALUMINIUM ZE STOPU Ti-6Al-4V

In the paper, results of a kinetic analysis of aluminium evaporation from the Ti-6Al-4V alloy are presented. The analysis was performed based on the findings obtained during the alloy smelting in the vacuum induction furnace at 5 Pa to 1000 Pa and at 1973 K, 1998 K and 2023 K.

Keywords: Ti-6Al-4V alloy, evaporation, kinetics, vacuum induction melting

W prezentowanej pracy przedstawiono wyniki analizy kinetycznej procesu parowania aluminium ze stopu Ti-6Al-4V. Przeprowadzono ją w oparciu o wyniki badań uzyskane w trakcie topienia stopu w indukcyjnym piecu próżniowym w zakresie ciśnień 5-1000 Pa w temperaturach 1973 K, 1998 K i 2023 K.

1. Introduction

One of the main conditions of successful metallurgical industry growth is constant development of new metal products with a potential for their implementation until 2030 as well as improvement of the existing product properties. Examples of new, modern materials are light titanium-based alloys. Their properties make them extremely interesting for aerospace, automotive and building industries as well as for broadly-taken biomedical engineering. Currently, a lot of research centres are still working on production technologies regarding new alloys from this group as well as on modernisation of their processing technology aimed at creating new potentials for their application. One of the basic components of titanium alloys is aluminium. With respect to titanium, this metal shows higher vapour pressures, which frequently results in serious problems during smelting of these alloys. This is related to possible disadvantageous Al evaporation during smelting and casting, which may lead to an alloy whose composition differs from the initially assumed composition. To prevent this process, it is necessary to understand the kinetics of aluminium evaporation from these alloys in terms of the stages that determine the process rate. In the paper, results of a kinetic analysis of aluminium evaporation from the Ti-6Al-4V alloy are presented. Based on the review of literature regarding aluminium evaporation from the Ti-Al-X alloys, the following may be concluded:

- The literature lacks a kinetic analysis of the process based on results of experimental studies conducted for a wide range of working pressures in smelting systems.
- The existing experimental data are rare and mainly relate to smelting with the use of ISM or EBM method [1 -13].
- No results of experiments conducted in conventional, vacuum induction furnaces (the VIM methodology) [14-16] are available.
- In the literature, various mathematical models can be found that allow for estimating the rates of aluminium evaporation from titanium alloys, but they have been verified with the use of a small number of experimental findings which, importantly, referred to very high vacuum conditions, i.e. $\leqslant$ 1Pa [2-4, 6].

2. Research methodology

The subject of investigations was the Ti-6Al-4V alloy (Grade 5 titanium) which, in addition to titanium, contained 5.50%mass aluminium, 3.77%mass vanadium and trace amounts of other elements.

The smelting experiments were performed with the use of a VIM 20-50 vacuum induction furnace manufactured by SECO-WARWICK. The furnace is presented in Fig. 1.

During the experiment, a 1000 g alloy sample was placed in the graphite melting pot (inner diameter: 90 mm; operating height: 220 mm) which was mounted inside the furnace induction coil. After closing the furnace chamber, the required pressure was generated by cooperating vacuum pumps (mechanical, Roots and diffusion pumps). When the assumed level of vacuum was reached, the charge material was heated up to the set temperature. The liquid metal was held at the set temperature for 600 sec. The temperature was measured with the

* SILESIAN UNIVERSITY OF TECHNOLOGY, FACULTY OF MATERIALS ENGINEERING AND METALLURGY, DEPARTMENT OF METALLURGY, 8 KRASIŃSKIEGO STR., 40-019 KATOWICE, POLAND

use of a pyrometer and a PtRh-Pt thermocouple. During the experiment, liquid metal samples were collected and subjected to a chemical analysis. When the test was completed, the liquid metal was poured into the ingot mould. When it solidified and the furnace cooled down, the vacuum chamber was opened. The metal cast was also subjected to the chemical analysis.

Fig. 1. The vacuum induction furnace used for the experiments

The experiments were performed at 5 Pa to 1000 Pa and at 1973 K, 1998 K, 2023 K. Examples of aluminium concentration changes in the Ti-6Al-4V alloy during the smelting process are presented in Fig. 2.

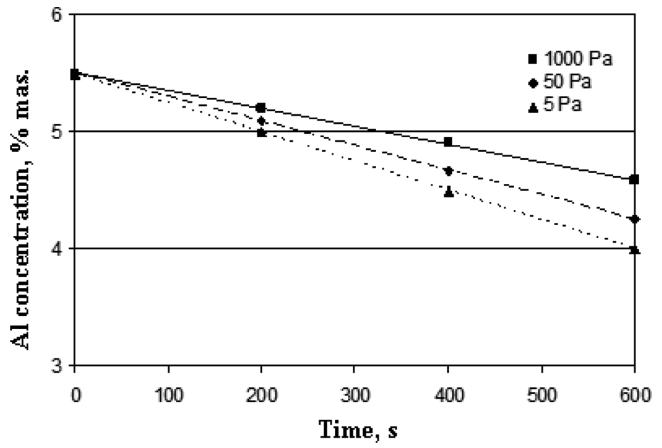

Fig. 2. Aluminium concentration changes during the Ti-6Al-4V alloy melting at 1998 K and 1000 Pa, 50 Pa and 5 Pa

3. The kinetic analysis of aluminium evaporation process

In the process of liquid metal alloy component evaporation, there are three essential stages [17, 18]:

- transfer of the evaporating component mass from the body of the liquid metal phase to the interface
- a surface reaction, i.e. the evaporation process on the liquid metal-gaseous phase interface – the gaseous phase
- transfer of the evaporating component mass from the interface to the core of gaseous phase

The overall flow of aluminium that is transferred from the liquid alloy body to the gaseous phase core can be described by the following equation:

$$N_{Al} = \left(\frac{1}{\beta^l_{Al}} + \frac{1}{\beta^g_{Al}} + \frac{1}{k^e_{Al}} \right)^{-1} \cdot C_{Al} \tag{1}$$

or

$$N_{Al} = k_{Al} \cdot C_{Al} \tag{2}$$

where:

k_{Al} – overall aluminium mass transfer coefficient,

$ß^l_{Al}$ – aluminium mass transfer coefficient in the liquid phase (titanium bath),

k^e_{Al} – aluminium evaporation rate constant,

$ß^g_{Al}$ – aluminium mass transfer coefficient in the gaseous phase,

C_{Al} – concentration.

The k_{Al} is described by the following equation [15]:

$$\frac{1}{k_{Al}} = \frac{1}{\beta^l_{Al}} + \frac{1}{\phi k^e_{Al}} + \frac{RT}{\varphi \beta^g_{Al}} \tag{3}$$

where:

$$\phi = \frac{p^o_{Al} \cdot \gamma_{Al} \cdot M_{Ti}}{\rho_{Ti}} \tag{4}$$

and:

T – temperature,

R – gas constant,

γ_{Al} – coefficient of Al activity in the alloy,

M_{Ti} – titanium molar mass,

ρ_{Ti} – liquid titanium density.

In order to determine the overall aluminium mass transfer coefficient based on the experimental data, the process rate was described by the following equation:

$$2.303 \log \frac{C^t_{Al}}{C^o_{Al}} = -k_{Al} \cdot \frac{F}{V}(t - t_o) \tag{5}$$

where:

F – evaporation areas (the interface)

V – liquid metal volume

$(t - t_o)$ – process duration.

With the use of equation (5), values of the overall aluminium mass transfer coefficient, k_{Al}, in the analysed evaporation process, were determined. The evaporation area (the area of liquid alloy), used for the calculations, was $63.59 \cdot 10^{-4} m^2$. The determined k_{Al} values are presented in Table 1.

To determine the contribution of resistance related to mass transfer in the liquid Ti-6Al-4V alloy to the overall resistance of the process, the value of mass transfer coefficient, $ß^l_{Al}$, is necessary. It is determined with the use of Machlin's

equation [19] which describes mass transfer in the liquid, inductively stirred metal phase:

$$\beta_{Al}^{l} = \left(\frac{8D_{Al} \cdot V_m}{\pi \cdot r_m}\right)^{\frac{1}{2}} \tag{6}$$

where:

v_m– near-surface velocity of inductively stirred liquid metal,

r_m – radius of the liquid metal surface (assumed to be the melting pot inner radius),

D_{Al} – Al diffusion coefficient in the liquid alloy.

Based on equation (6), it is seen that for the β_{Al}^{l} estimation, the near-surface velocity of liquid metal must be known. Many studies have shown that the v_m value depends on a lot of factors, i.e. density and viscosity of the metal as well as the electrical parameters of furnace operation, including current frequency, device power and current intensity in the induction coil. Another important factor is a position of the melting pot in relation to the inductor [20, 21].

For the investigated Ti-6Al-4V alloy, the following equation [10] was used to determine the values of near-surface velocity, v_m:

$$v_m = v_1 + (v_2 - v_1) \cdot \frac{(T - T_1)}{300} \tag{7}$$

assuming that, respectively, $v_1 = 0.06$ m·s^{-1}, $v_2 = 0.21$ m·s^{-1} and $T_1 = 1933$ K (the alloy melting temperature).

The near-surface velocities of liquid Ti-6Al-4V alloy, determined with the use of equation (7), were 0.080 m·s^{-1} at 1973 K, 0.093 m·s^{-1} at 1998 K and 0.105 m·s^{-1} at 2023 K.

In order to determine the coefficient of aluminium diffusion in the liquid phase, the following equation [3] was used:

$$D_{Al} = 10^{-8} \exp\left[\frac{250000}{R}\left(\frac{1}{1925} - \frac{1}{T}\right)\right] \tag{8}$$

In Table 2, values of the coefficient of mass transfer in the liquid phase, determined with the use of equation (6), are presented.

For the analysis of the rate of liquid phase-gaseous phase transition, which occurs on the interface, it should be taken into account that the maximum mass flow of the component that evaporates from the liquid metal surface to the gaseous phase is determined by the Langmuir-Knudsen equation:

$$N_i^e = \frac{\alpha(p_{ieq} - p_{is})}{(2\pi RTM_i)^{0.5}} \tag{9}$$

Based on this equation, the evaporation rate constant can be determined:

$$k^e = \frac{\alpha}{(2\pi RTM_i)^{0.5}} \tag{10}$$

However, the equation is only true in the case of so-called "absolute vacuum". In Table 1, the estimated values of substitutional evaporation rate constant, $k_{Al}^{e'}$, determined by the following equation, are presented:

$$k_{Al}^{e'} = k_{Al}^{e} \cdot \phi \tag{11}$$

The values of liquid metal density were calculated with the use of the following equation [22]:

$$\rho_{Ti} = 4.208 - 5.08 \cdot 10^{-4} \cdot (T - 1941) \tag{12}$$

TABLE 1

The values of overall mass transfer coefficient, coefficient of the mass transfer in the liquid phase and substitutional evaporation rate constant for the process of aluminium evaporation from the Ti-6Al-4V alloy

Experiment no.	Experiment conditions	Overall mass transfer coefficient, k_{Al} m·s^{-1}	Mass transfer coefficient in the liquid phase, β_{Al}^{l} m·s^{-1}	Substitutional evaporation rate constant $k_{Al}^{e'}$ m·s^{-1}
1	Al-1973-1000	$1.07 \cdot 10^{-5}$	$2.57 \cdot 10^{-4}$	$1.90 \cdot 10^{-5}$
2	Al -1973-1000	$0.97 \cdot 10^{-5}$	$2.57 \cdot 10^{-4}$	$1.90 \cdot 10^{-5}$
3	Al -1973-1000	$0.94 \cdot 10^{-5}$	$2.57 \cdot 10^{-4}$	$1.90 \cdot 10^{-5}$
4	Al -1998-1000	$1.25 \cdot 10^{-5}$	$3.04 \cdot 10^{-4}$	$2.37 \cdot 10^{-5}$
5	Al -1998-1000	$1.15 \cdot 10^{-5}$	$3.04 \cdot 10^{-4}$	$2.37 \cdot 10^{-5}$
6	Al -1998-1000	$1.20 \cdot 10^{-5}$	$3.04 \cdot 10^{-4}$	$2.37 \cdot 10^{-5}$
7	Al -2023-1000	$1.51 \cdot 10^{-5}$	$3.56 \cdot 10^{-4}$	$2.97 \cdot 10^{-5}$
8	Al -2023-1000	$1.59 \cdot 10^{-5}$	$3.56 \cdot 10^{-4}$	$2.97 \cdot 10^{-5}$
9	Al -2023-1000	$1.54 \cdot 10^{-5}$	$3.56 \cdot 10^{-4}$	$2.97 \cdot 10^{-5}$
10	Al -1973-100	$1.48 \cdot 10^{-5}$	$2.57 \cdot 10^{-4}$	$1.90 \cdot 10^{-5}$
11	Al -1973-100	$1.48 \cdot 10^{-5}$	$2.57 \cdot 10^{-4}$	$1.90 \cdot 10^{-5}$
12	Al -1973-100	$1.43 \cdot 10^{-5}$	$2.57 \cdot 10^{-4}$	$1.90 \cdot 10^{-5}$
13	Al -1998-100	$1.57 \cdot 10^{-5}$	$3.04 \cdot 10^{-4}$	$2.37 \cdot 10^{-5}$
14	Al -1998-100	$1.57 \cdot 10^{-5}$	$3.04 \cdot 10^{-4}$	$2.37 \cdot 10^{-5}$
15	Al -1998-100	$1.57 \cdot 10^{-5}$	$3.04 \cdot 10^{-4}$	$2.37 \cdot 10^{-5}$
16	Al -2023-100	$1.64 \cdot 10^{-5}$	$3.56 \cdot 10^{-4}$	$2.97 \cdot 10^{-5}$
17	Al -2023-100	$1.62 \cdot 10^{-5}$	$3.56 \cdot 10^{-4}$	$2.97 \cdot 10^{-5}$
18	Al -2023-100	$1.62 \cdot 10^{-5}$	$3.56 \cdot 10^{-4}$	$2.97 \cdot 10^{-5}$
19	Al -1973-50	$1.52 \cdot 10^{-5}$	$2.57 \cdot 10^{-4}$	$1.90 \cdot 10^{-5}$
20	Al -1973-50	$1.52 \cdot 10^{-5}$	$2.57 \cdot 10^{-4}$	$1.90 \cdot 10^{-5}$
21	Al -1973-50	$1.50 \cdot 10^{-5}$	$2.57 \cdot 10^{-4}$	$1.90 \cdot 10^{-5}$
22	Al -1998-50	$1.62 \cdot 10^{-5}$	$3.04 \cdot 10^{-4}$	$2.37 \cdot 10^{-5}$
23	Al -1998-50	$1.74 \cdot 10^{-5}$	$3.04 \cdot 10^{-4}$	$2.37 \cdot 10^{-5}$
24	Al -1998-50	$1.71 \cdot 10^{-5}$	$3.04 \cdot 10^{-4}$	$2.37 \cdot 10^{-5}$
25	Al -2023-50	$1.65 \cdot 10^{-5}$	$3.56 \cdot 10^{-4}$	$2.97 \cdot 10^{-5}$
26	Al -2023-50	$1.75 \cdot 10^{-5}$	$3.56 \cdot 10^{-4}$	$2.97 \cdot 10^{-5}$
27	Al -2023-50	$1.72 \cdot 10^{-5}$	$3.56 \cdot 10^{-4}$	$2.97 \cdot 10^{-5}$
28	Al -1973-10	$1.52 \cdot 10^{-5}$	$2.57 \cdot 10^{-4}$	$1.90 \cdot 10^{-5}$
29	Al -1973-10	$1.52 \cdot 10^{-5}$	$2.57 \cdot 10^{-4}$	$1.90 \cdot 10^{-5}$
30	Al -1973-10	$1.51 \cdot 10^{-5}$	$2.57 \cdot 10^{-4}$	$1.90 \cdot 10^{-5}$

31	Al -1998-10	$1.86 \cdot 10^{-5}$	$3.04 \cdot 10^{-4}$	$2.37 \cdot 10^{-5}$
32	Al -1998-10	$1.95 \cdot 10^{-5}$	$3.04 \cdot 10^{-4}$	$2.37 \cdot 10^{-5}$
33	Al -1998-10	$1.90 \cdot 10^{-5}$	$3.04 \cdot 10^{-4}$	$2.37 \cdot 10^{-5}$
34	Al -2023-10	$1.94 \cdot 10^{-5}$	$3.56 \cdot 10^{-4}$	$2.97 \cdot 10^{-5}$
35	Al -2023-10	$1.93 \cdot 10^{-5}$	$3.56 \cdot 10^{-4}$	$2.97 \cdot 10^{-5}$
36	Al -2023-10	$1.93 \cdot 10^{-5}$	$3.56 \cdot 10^{-4}$	$2.97 \cdot 10^{-5}$
37	Al -1973-5	$1.61 \cdot 10^{-5}$	$2.57 \cdot 10^{-4}$	$1.90 \cdot 10^{-5}$
38	Al -1973-5	$1.62 \cdot 10^{-5}$	$2.57 \cdot 10^{-4}$	$1.90 \cdot 10^{-5}$
39	Al -1973-5	$1.62 \cdot 10^{-5}$	$2.57 \cdot 10^{-4}$	$1.90 \cdot 10^{-5}$
40	Al -1998-5	$1.93 \cdot 10^{-5}$	$3.04 \cdot 10^{-4}$	$2.37 \cdot 10^{-5}$
41	Al -1998-5	$1.98 \cdot 10^{-5}$	$3.04 \cdot 10^{-4}$	$2.37 \cdot 10^{-5}$
42	Al -1998-5	$1.99 \cdot 10^{-5}$	$3.04 \cdot 10^{-4}$	$2.37 \cdot 10^{-5}$
43	Al -2023-5	$1.95 \cdot 10^{-5}$	$3.56 \cdot 10^{-4}$	$2.97 \cdot 10^{-5}$
44	Al -2023-5	$2.03 \cdot 10^{-5}$	$3.56 \cdot 10^{-4}$	$2.97 \cdot 10^{-5}$
45	Al -2023-5	$2.03 \cdot 10^{-5}$	$3.56 \cdot 10^{-4}$	$2.97 \cdot 10^{-5}$

4. Discussion of results

As demonstrated by the results of experimental Ti-6Al-4V alloy smelting in the vacuum induction furnace, the temperature rise from 1973 K to 2023 K and the working pressure reduction from 1000 Pa to 5 Pa are accompanied by higher aluminium loss from 14% to 28% compared to its initial content in the alloy. At the same time, the value of overall mass transfer coefficient, k_{Al}, increases from $0.94 \cdot 10^{-5}$ $m \cdot s^{-1}$ to $2.03 \cdot 10^{-5}$ $m \cdot s^{-1}$.

Based on the analysis of pressure effects on the investigated evaporation process, it can be demonstrated that the vacuum rise in the device leads to markedly higher aluminium elimination rate, which is illustrated by the data presented in Fig. 3.

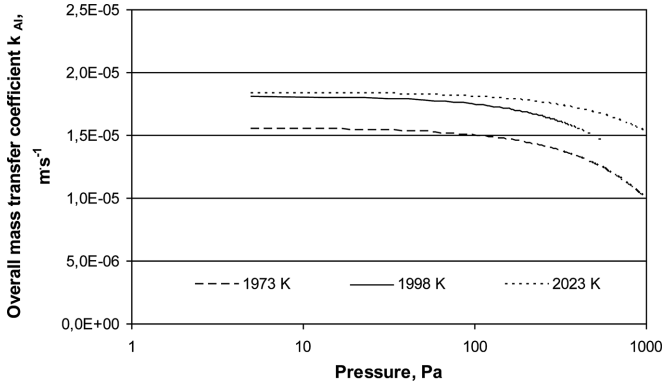

Fig. 3. Value changes of the overall mass transport coefficient, k_{Al}, depending on the furnace working pressure

The determined values of k_{Al}, mass transfer coefficient in the liquid phase (β^l_{Al}) and the substitutional evaporation rate constant ($k^{e'}_{Al}$) are clearly positioned in the following rank:

$$k_{Al} < k^{e'}_{Al} < \beta^l_{Al} \tag{13}$$

It is illustrated by the data presented in Figs. 4-5.

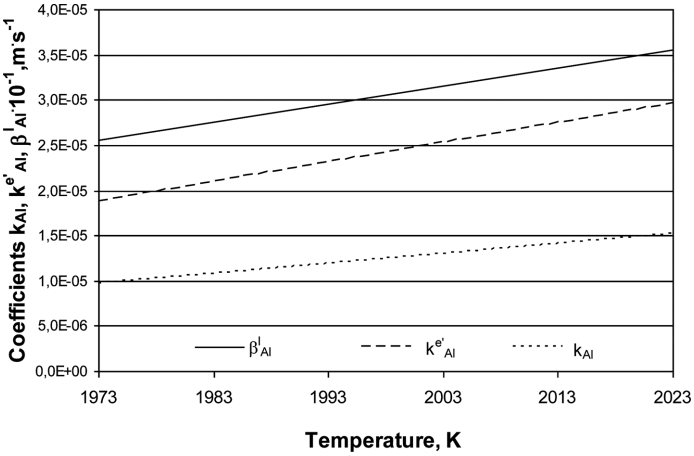

Fig. 4. Values of k_{Al}, β^l_{Al} and $k^{e'}_{Al}$ versus temperature, determined based on the own investigations (p = 1000 Pa)

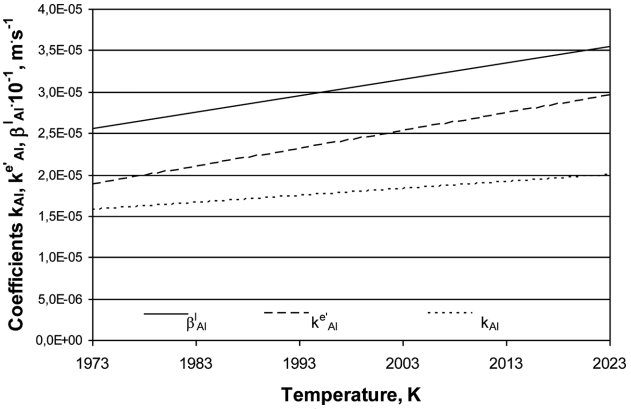

Fig. 5. Values of k_{Al}, $ß^l_{Al}$ and $k^{e'}_{Al}$ versus temperature, determined based on the own investigations (p = 5 Pa)

The presented relations are consistent with findings obtained by the authors of [7] for the process of aluminium evaporation from the Ti-Al alloy (34%mass) that is smelted with the use of ISM technology. They are presented in Fig. 6.

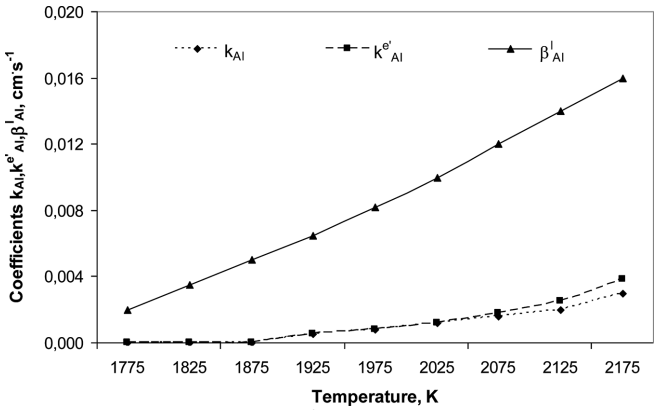

Fig. 6. Values of k_{Al}, β^l_{Al} and $k^{e'}_{Al}$ versus temperature for aluminium evaporation from the Ti-Al alloy (34%mass Al); p= 13.3 [7]

The determined k_{Al}, β^l_{Al} *and* $k^{e'}_{Al}$ values allowed for defining the stages that determined the investigated process. The

contribution of resistance related to mass transfer in the liquid phase was determined with the use of following equation:

$$U_l = \frac{\frac{1}{\beta^l_{Al}}}{\frac{1}{k_{Al}}} \cdot 100\% \tag{14}$$

Analogically, resistance related to the evaporation itself was determined:

$$U_e = \frac{\frac{1}{k^{e'}_{Al}}}{\frac{1}{k_{Al}}} \cdot 100\% \tag{15}$$

The contribution of resistance related to mass transfer in the liquid phase did not exceed 7% for the whole pressure range. At the same time, the contribution of resistance related to the evaporation process, U_e, to the overall process resistance for the whole pressure range exceeded 50%, which means that the investigated process was kinetically controlled. The summary resistance $\left(\frac{1}{k^{e'}_{Al}} + \frac{1}{\beta^l_{Al}}\right)$ accounted for 54% to 91% of the overall process resistance. It is illustrated by the data presented in Figs. 7-8. Figures 9-10 present a comparison of the resistances calculated based on the own study and based on the studies conducted by Su, Guo, Jia, Liu and Liu [7].

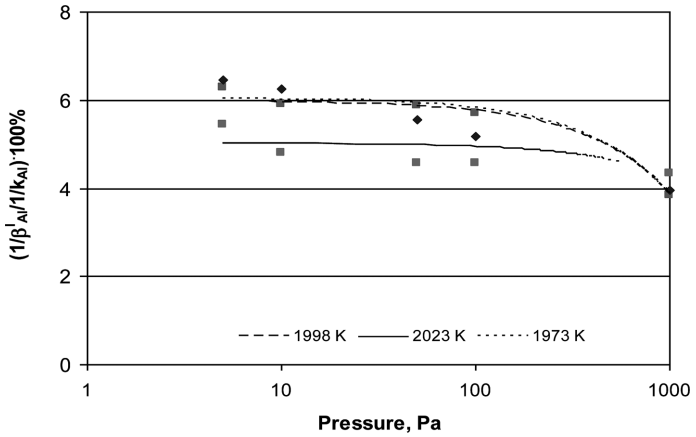

Fig. 7. Value changes of the contribution of resistance in the liquid phase to the overall process resistance depending on the pressure

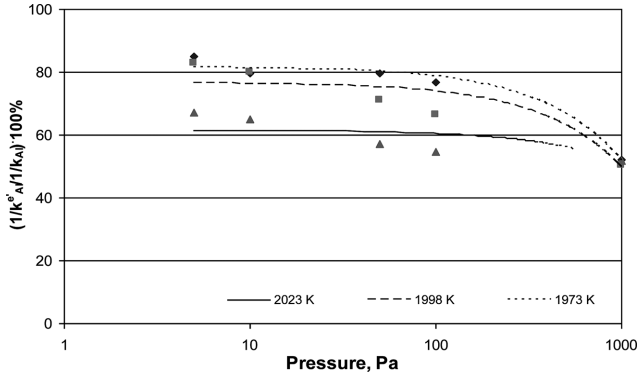

Fig. 8. Value changes of the contribution of resistance related to evaporation to the overall process resistance depending on the pressure

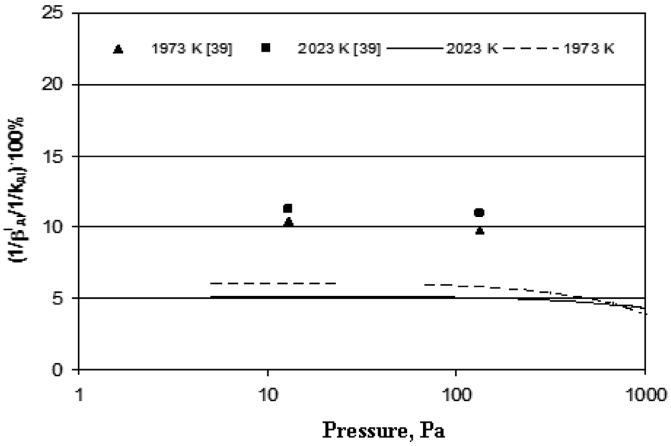

Fig. 9. Comparison of the contributions of resistance in the liquid phase to the overall process resistance determined based on the own study and based on the studies conducted by Su et al. [7]

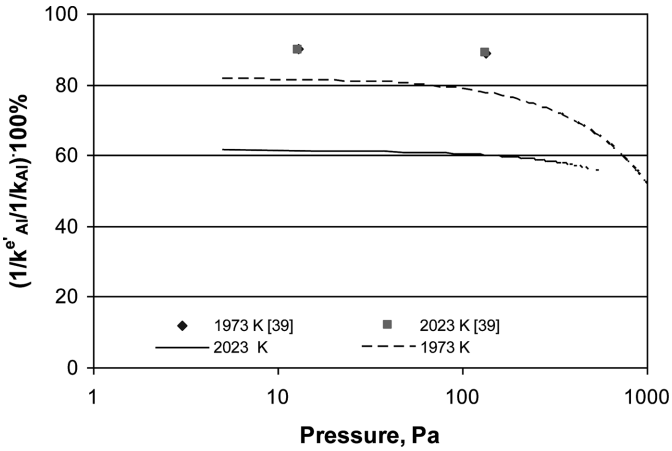

Fig. 10. Comparison of the contributions of resistance related to evaporation to the overall process resistance determined based on the own study and based on the studies conducted by Su et al. [7]

To confirm that the investigated process is kinetically controlled, the value of its activation energy was determined by means of the Arrhenius equation:

$$\ln k_{Al} = \frac{-E_A}{R \cdot T} \tag{16}$$

where:

E_A – activation energy of the process.

For all working pressures, the estimated activation energies are far above 100 kJ/mol, which is typical of kinetically controlled processes. For instance, the activation energies for 100 Pa, 10 Pa and 5 P are 200 kJ/mol, 161 kJ/mol and 143 kJ/mol, respectively.

In the case of diffusion control in the liquid phase, these values are much smaller and comparable to the diffusion activation energies in liquids. For example, the diffusion activation energy value for cobalt and iron in liquid copper is 11 kJ/mol, while for chromium, nickel, manganese and vanadium in liquid iron, it ranges from 15 to 25 kJ/mol.

5. Conclusions

Based on the experimental results of Ti-6Al-4V smelting in the vacuum induction furnace at 5–1000 Pa and 1973–2023 K as well as on the kinetic analysis findings, it was demonstrated that:

- During smelting, aluminium is eliminated through its evaporation.
- The furnace working pressure reduction from 1000 Pa to 5 Pa and temperature rise from 1973 K to 2023 K are accompanied by aluminium loss from the alloy from 14% to 28% compared to the initial concentration (5.5%mass). At the same time, the value of overall mass transfer coefficient, k_{Al}, increases from $0.94 \cdot 10^{-5}$ m$\cdot$ s^{-1} to $2.03 \cdot 10^{-5}$ m$\cdot$s^{-1}.
- Kinetically, it was shown that for the whole pressure range, the contribution of resistance related to mass transfer in the liquid phase to the overall process resistance did not exceed 7%.
- The stage that determines the investigated process within the analysed pressure and temperature ranges is a reaction on the liquid metal surface (evaporation), which means that the process is kinetically controlled. It is confirmed by the determined values of activation energy of the process which are over 140 kJ/mol.
- The summary resistance related to both mass transfer in the liquid phase and the evaporation process is higher than 54% of the overall process resistance.

Acknowledgements

The study was conducted under the Research Project No. N N508 589439, financed by the Ministry of Science and Higher Education – Poland.

REFERENCES

[1] S. Watakabe, K. Suzuki, K. Nishikawa, Control of chemical compositions of Ti-6Al-4V alloy during melting by electron beam furnace, ISIJ International **32** (5), 625-629 (1992).

[2] S.V. Akhonin, N.P. Trigub, V.N. Zamkov, S.L. Siemiatin, Mathematical modeling of aluminum evaporation during electron-beam cold-hearth melting of Ti-6Al-4V ingots, Metallurgical and Materials Transactions B **34** B, 447-453 (2003).

[3] S.L. Semiatin, V.G. Ivanchenko, S.V. Akhonin, O.M. Ivasishin, Diffusion models for evaporation losses elektron-beam melting of alpha/beta-titanium alloys, Metallurgical and Materials Transactions B **35B**, 235-245 (2004).

[4] A. Powell, J. Van Den Avyle, B. Damkroger, J. Szekely, U. Pal, Analysis of multicomponent evaporation in electron beam melting and refining of titanium alloys, Metallurgical and Materials Transactions B **28 B**, 1227-1239 (1997).

[5] H. Nakamura, A. Mitchell, The effect of beam oscillation rate on Al evaporation from a Ti-6Al-4V alloy in the electron beam melting process, ISIJ International **32** (5), 583-592 (1992).

[6] V. Ivanchenko, G. Ivasishin, S. Semiatin, Evaluation of evaporation losses during electron-beam melting of Ti-Al-V alloys, Metallurgical and Materials Transactions B **34 B**, 911-915 (2003).

[7] Y. Su, J. Guo, J. Jia, G. Liu, Y. Liu, Composition control of a TiAl melt during the induction skull melting (ISM) process, Journal of Alloys and Compounds **334**, 261-266 (2002).

[8] J. Guo, G. Liu, Y. Su, H. Ding, J. Jia, H. Fu, The critical pressure and impeding pressure of Al evaporation during induction skull melting processing of TiAl, Metallurgical and Materials Transactions A **31 A**, 3249-3253 (2002).

[9] J. Guo, Y. Liu, Y. Su, H. Ding, G. Liu, J. Jia, Evaporation behavior of aluminum during the cold crucible induction skull melting of titanium aluminum alloys, Metallurgical and Materials Transactions B **31 B**, 837-844 (2000).

[10] J. Guo, G. Liu, Y. Su, H. Ding, J. Jia, H. Fu, Evaporation of multi-components in Ti-25Al-25Nb melt during induction skull melting process, Transactions of Nonferrous Metals Society of China **12** (4), 587-591 (2002).

[11] G. Liu, Y. Su, J. Guo, H. Ding, J. Jia, H. Fu, Evaporation loss of the components in Ti-13Al-29Nb-2.5Mo melt during ISM process, Rare Metal, Materials and Engineering **32** (2), 108-122 (2003).

[12] G. Liu, Y. Su, J. Guo, H. Ding, J. Jia, H. Fu, Evaporation loss of components during induction skull melting of Ti-13Al-29Nb-2.5Mo, International Journal of Cast Metals Research **16** (5), 466-472 (2003).

[13] J. Guo, G. Liu, Y. Su, H. Ding, J. Jia, H. Fu, Control of Al content during ISM process of Nb_3Al, Transactions of Nonferrous Metals Society of China **10** (5), 571-574 (2000).

[14] L. Blacha, R. Burdzik, A. Smalcerz, T. Matuła, Effects of pressure on the kinetics of manganase evaporation from the OT 4 alloy, Archives of Metallurgy and Materials **58** (1), 197-201 (2013).

[15] L. Blacha, J. Mizera, P. Folęga, The effects of mass transfer in the liquid phase on the rate of aluminium evaporation from the Ti-6Al-7Nb alloy, Metalurgija **53** (1), 51-54 (2014).

[16] G. Siwiec, Elimination of aluminum during the process of Ti-6Al-4V alloy during in a vacuum induction furnace, Archives of Metallurgy and Materials **57** (4), 951-956 (2012).

[17] L. Blacha, Bleientfernung aus kupferlegierungen im prozess der vakuumraffination, Archives of Metallurgy **48** (1), 105-127 (2003).

[18] L. Blacha, Untersuchungen der antimonentfernungsgeschwindigkeit aus blisterkupfer im prozess der vakuumraffination, Archives of Metallurgy and Materials **50** (4), 989-1002 (2005).

[19] R.G. Ward, Evaporative losses during vacuum induction melting of steel, Journal of the Iron and Steel Inst. **201**, 920-923 (1963).

[20] L. Blacha, J. Łabaj, Factors determining of the proces sof metal bath components evaporation, Metalurgija **51** (4), 529-533 (2012).

[21] J. Łabaj, Kinetics of coper evaporation from the Fe-Cu alloys under reduced pressure**,** Archives of Metallurgy and Materials **57** (1), 165-172 (2012).

[22] H.P. Wang, S.J. Yang, B.B. Wei, Density and structure of undercooled liquid titanium, Chinese Science Bulletin **57**, 719-723 (2012).

Received: 10 April 2012.